 doi:10.20944/preprints202103.0361.v1

Type of the Paper (Article, Review, Communication, etc.)

Poly (Lactic Acid) (PLA) / Ground Tire Rubber (GTR) Blends Using Peroxide Vulcanization

Nicolas Candau [1,*], Oguzhan Oguz [2,3], Noel León Albiter [1], Gero Förster [1], Maria Lluïsa Maspoch [1]

[1] Centre Català del Plàstic (CCP) - Universitat Politècnica de Catalunya Barcelona Tech (EEBE-UPC), Av. D'Eduard Maristany, 16, 08019, Spain
[2] Faculty of Engineering and Natural Sciences, Materials Science and Nano Engineering, Sabanci University, 34956, Orhanli, Tuzla, Istanbul, Turkey
[3] Sabanci University Integrated Manufacturing Technologies Research and Application Center & Composite Technologies Center of Excellence, Teknopark Istanbul, 34906 Pendik, Istanbul, Turkey
* Correspondence: nico.candau@gmail.com

Abstract: Poly (Lactic Acid) (PLA) / Ground Tire Rubber (GTR) blends using Dicumyl peroxide (DCP) as a crosslinking agent were prepared as a route to recycle wastes rubber from the automotive industry. The GTR were exposed to grinding and exhibited mechanical damage, traduced at the rubber network scale by chains scission and/or chemical cross-links breakage. Such damage is accompanied by a decrease of 80% of the rubber chains network density of the initial tire buffing but found independent on the type of grinding (cryogenic, dry ambient) or on the GTR size (from <400 μm to <63 μm). Moreover, the finest sieved GTR contain the largest the amount of reinforcing elements (carbon black, clay) that can be advantageously used in PLA/GTR blends. The melt-blending of these finest GTR particles obtained by cryo-grinding at an amount of 15 wt.% and in presence of the crosslinking agent (DCP), resulted in an optimum improvement of the ductility, energy at break and impact strength of the PLA/GTR blends as compared to neat PLA, while maintaining its stiffness. The results were attributed to (i) the good dispersion of the fine GTR particles into the PLA matrix, (ii) the partial re-crosslinking of the GTR particles and co-crosslinking at PLA/GTR interface and (iii) the presence of reinforcing carbon black into the GTR particles and clay particles dispersed into the PLA matrix.

Keywords: Poly (Lactic Acid) (PLA); wastes rubber; recycling; tensile properties

1. Introduction

Due to the generation of mega-tons of plastics and rubber wastes each year in Europe, the polymer industry is facing a considerable ecological risk [1]. To tackle this issue, the recycling of wastes rubber [2],[3] and the elaboration of bio-based plastics [4],[5] have shown a wide development within the last decade. By using these ecological strategies, thermoplastic elastomers (TPE) [6],[7],[8],[9],[10] using conventional thermoplastics from crude oil (PE, PP, PET) and fresh elastomers (EPDM, NR, SBR) were progressively replaced by polymeric blends containing bio-based thermoplastics [11],[12],[13], wastes thermoplastics [14],[15] or wastes rubber [16],[17]. Initially based on an ecological demand, the industrial production of these green materials also requires mechanical performances (stiffness, strength, ductility) comparable to the ones of conventional thermoplastic elastomers they intend to replace.

The progressive replacement of fresh rubber by Ground Tire Rubber (GTR) in TPE aims to participate in the circular economy of the automotive industry. Nonetheless, these blends generally contain a limited quantity of wastes rubber as thermoplastic properties rapidly deteriorate at GTR amounts of 10-20 wt.% of GTR [18],[19]. This is due to the presence of large rubber particles [20] and their facility to aggregate due to their weak miscibility and poor interfacial adhesion with the plastic phase [21]. The interfacial properties between GTR and the plastic matrix can however be drastically improved by reducing the

Preprints (www.preprints.org) | NOT PEER-REVIEWED | Posted: 15 March 2021 doi:10.20944/preprints202103.0361.v1

GTR particle size [21],[22], by using compatibilizers [22],[23],[24] and vulcanizing agents [24],[25],[26] or encapsulating wastes rubber into a fresh rubber phase [17],[23].

Several investigations have been conducted to improve the properties of TPE containing bio-based thermoplastics such as PLA. PLA had been blended with natural fibers [27],[28],[29], toughening polymers [30],[31] in presence of reactive compatibilizers [32],[33] or using dynamic vulcanization [34],[35]. It has been shown that, in absence of vulcanizing agent, the drastic reduction of rubber particles down to several nanometers into a PLA matrix resulted in a significant improvement of the tensile toughness without compromising stiffness and strength [36]. While of interest to improve the tensile properties of the brittle PLA, the latter method shows some limitation as a possible route to rubber recycling as it re-uses a limited amount of rubber.

The degradability of PLA by main chain scission [37] and of wastes rubber by reversion of polysulfide bonds [38],[39], make the preparation of bio-based PLA and wates rubber (GTR) challenging [40],[41],[42],[43]. Scrap rubber from tires after thermal shock method [40] and frost shattering method [41] were blended with PLA. Tensile and impact properties of PLA were found to be lowered by wastes rubber addition due to poor adhesion between the wastes rubber and PLA matrix. However, the use of silane agent as compatibilizer in PLA/GTR blends showed increased strain at fail and impact strength while elastic modulus and strength decreased moderately for an optimal GTR content of 15 wt.% [42],[43]. Finally, the use of a vulcanizing agent, had been demonstrated to show significant improvement of mechanical properties of PLA/Natural Rubber (NR) blends [44],[45],[46], but has not been investigated yet in PLA/GTR blends.

This study presents an investigation dedicated to the preparation of PLA-GTR blends using DCP as a crosslinking agent. A systematic study has been conducted regarding the role of GTR particle size, the type of GTR grinding process, the DCP influence and the quantity of wastes rubber introduced into the PLA/GTR blends. In the first section, the properties of the GTR particles were studied. Their composition, size distribution and crosslink density were discussed which allowed to make a careful selection of the GTR particles for further blending with PLA. In the second and third sections, the tensile and impact properties of the PLA-GTR blends were presented. It has been found that the addition of 15 wt.% of the finest cryo-grinded GTR in presence of DCP showed the least decrease of the strength, a maintain of the elastic modulus, the most improved ductility, energy at break and impact strength as compared to neat PLA.

2. Materials and Methods

2.1. Materials composition

The PLA2002D® extrusion grade was obtained from NatureWorks. Ground tire rubber (GTR) was supplied by the company J. Allcock & Sons Ltd using the transformation of tire buffing into finer rubber crumbs via a controlled dry-ambient grinding (GTR_a) or cryo-grinding (GTR_c). The obtained GTR contains rubber and carbon black (CB). The rubber is composed of Natural Rubber (NR) and Styrene Butadiene Rubber (SBR). The GTR particles were subsequently separated into different sizes using a vibratory sieve shaker (Analysette 3). The sieving was performed during 5 minutes in dry conditions with a vibratory amplitude of 0.15 mm. The following sizes were extracted for the GTR_a: 40 ’s mesh (size < 420 μm), 80 ’s mesh (size < 180 μm) and 120 ’s mesh (size < 125 μm). For the cryo-grinded GTR_c, the following sizes were extracted: 120 ’s mesh (size < 125 μm) and 230 ’s mesh (size < 63 μm). The size distribution of the GTR particles was determined using an ImageJ treatment of optical microscopy images of the GTR particles. Before melt-blending, the PLA was dried overnight in a vacuum oven (Vaciotem-TV, J.P. SELECTA®) to prevent humidity absorption, over silica gel at 70 °C to remove any moisture. The sieved GTR crumbs were dried under the same conditions.

2.2. Materials processing

Melt blending was performed in an internal mixer (Brabender Plastic-Corder W50EHT, Brabender GmbH & Co.) using two counter-rotating screws (roller blade type

Preprints (www.preprints.org) | NOT PEER-REVIEWED | Posted: 15 March 2021 doi:10.20944/preprints202103.0361.v1

"W"). After optimisation of the processing conditions, the processing temperature was chosen equal to 170 °C and the rotation speed equal to 60 RPM. The PLA was first added, and an antioxidant (Irganox® 1010, BASF) was used (0.2 wt. % of the total weight of the PLA/GTR blend) to prevent PLA degradation during the blending. After 5 minutes (stabilization of the torque), the GTR rubber crumbs were added. 5 minutes after the introduction of GTR (stabilization of the torque), the dicumyl peroxide (DCP) is finally added (1.5 grams per hundred grams of GTR) as vulcanizing agent. The blends were then hot-pressed at 1 MPA and 170 °C during 5 minutes in a LAP PL-15 plate press (IQAP Masterbatch SL) using a mask of 1 mm thickness. The plate was subsequently cooled down to room temperature with a cooling rate of 50 °C.min^{-1}. Such fast cooling was chosen so that the obtained PLA/GTR do not re-crystallize (the DSC crystallinity was measured below 2 wt.% for all prepared blends).

Table 1. Code of the processed blends using various GTR grinding processes, sieving meshes and PLA/GTR quantities. All blends were prepared with 0.2 wt.% Irganox® 1010.

Sample code	GTR weight content (%)	DCP (per 100 g of GTR)	Pre-treatment of the GTR powder	Particles mesh size (µm)
PLA	0	-	-	-
PLA/GTR$_a$ 15% Y 's	15	1.5	Ambient grinding	Y=40 's; 80 's; 120 's
PLA/GTR$_a$ 15% Y 's	15	1.5	Ambient grinding	Y=40 's; 80 's; 120 's
PLA/GTR$_c$ 15% Y 's	15	1.5	Cryogenic grinding	Y=120 's; 230 's
PLA/GTR$_a$ X% 120 's	X=7.5;15;22.5	0	Ambient grinding	120 's
PLA/GTR$_a$ X% 120 's	X=7.5;15;22.5	1.5	Ambient grinding	120 's
PLA/GTR$_c$ X% 120 's	X=3;7.5;15;30	1.5	Cryogenic grinding	120 's
PLA/GTR$_c$ 15% 120 's	X=15	0	Cryogenic grinding	120 's

2.3. Scanning Electron Microscopy (SEM)

The fracture surfaces of the specimens were observed after tensile testing with a field emission scanning electron microscope (JSL-7001F, JEOL). A few nanometers thick conductive layer of a Pt_{80}/Pd_{20} alloy was sputtered on the fracture surface using a high-resolution sputter coater (Cressington 208HR) in order to avoid electron charging on the specimen surface. The surface topography was observed with a voltage of 1 kV. Chemical analysis was performed by EDX with a voltage of 20 kV.

2.4. Thermogravimetric analysis (TGA)

Thermogravimetric analysis is performed on GTR particles using a STAR^e system (Mettler Toledo). The particles are put into alumina crucible with a quantity around 5-10 mg. The standard IEC 60811-100 is used for the determination of the carbon black content. To do so, the GTR are heated from 30 °C to 1000 °C with a heating ramp of 10 °C/min working under nitrogen environment from 30 °C to 850 °C, and under air environment from 850 °C to 1000 °C.

2.5. Swelling

GTR is immersed in cyclohexane for 72 h and the solvent is changed every 24 h. After 72 h the swollen mass of (m_s) is measured. The GTR are then placed in an oven under vacuum at 70 °C during 6 h to remove the solvent. The mass of the dry samples (m_d) is

Preprints (www.preprints.org) | NOT PEER-REVIEWED | Posted: 15 March 2021 doi:10.20944/preprints202103.0361.v1

then measured. The swelling ratio of the specimen Q is calculated. The network chain density is calculated from swelling and the Flory-Rehner equation:

$$v = \frac{ln(1 - v_2) + v_2 + \chi_1 {v_2}^2}{V_1(-{v_2}^{\frac{1}{3}} + \frac{2}{f} v_2)} \quad (1)$$

With $v_) = 1/Q_B$. V_1=108 cm^3/mol^{-1} is the molar volume of the solvent (cyclohexane), c_1 is the Flory-Huggins polymer solvent dimensionless interaction term (c_1 is equal to 0.353 for the GTR-cyclohexane system). The ratio $2/f$ is associated with the phantom model that assumes spatial fluctuation of crosslinks (non-affine) used for high deformation ratios. f, the crosslink functionality, is chosen equal to 4. GTR contains non-rubber particles like carbon black. Hence, the Kraus correction [47] is used to account for the contribution of filler in swelling ratio, assuming that they do not contribute to swelling. Q_c is the swelling ratio of the rubber matrix defined as follows:

$$Q_c = \frac{Q - \varphi}{1 - \varphi} \quad (2)$$

with φ is the volume fraction of fillers. Krauss correction in Equation 2 assumes non-adhesion of the fillers to the rubbery matrix in the swollen state.

2.6. Thermoporosimetry

GTR is put into cyclohexane during 72 h to reach the swelling equilibrium. They are then carefully extracted and put into an aluminum crucible. A Q2000 DSC (TA Instruments) is used. The sample is first cooled down to -50 °C at 10 °C/min followed by an isothermal step at -50 °C during 2 min. The sample is then heated at 10 °C.min^{-1} up to 30 °C, during which endothermic peaks correspond to melting T_m of the cyclohexane entrapped in the network. Melting peaks are deconvoluted and the intensity is normalized by the swollen weight. The full procedure developed for vulcanized natural rubber [48],[49] and EPDM [50],[51] is used here for rubber particle wastes. By derivation of the Gibbs-Thompson equation, the normalized pore size is given by:

$$\frac{L}{L_f} = \frac{{T_m}^0 - T_f}{{T_m}^0 - T} \quad (3)$$

With T_f and L_f correspond to the melting temperature and the size of the largest pores entrapped in the network respectively. After derivation of equation 3, the normalized intensity distribution of the pore size is given by:

$$I_n = \frac{1}{m}\frac{dH}{dT}\frac{\left({T_m}^0 - T\right)^2}{L_f} \quad (4)$$

L_f value being unknown, the intensity $I=L_f I_n$ is hence plotted instead I_n to account for the pore size distribution. The average normalized pore size is then calculated as the L/L_f value associated with half of the area under the normalized signal.

2.7. Uniaxial Tensile Stretching (UTS)

Dogbone shaped specimens of type 1BA were extracted from hot moulded sheets by die-cutting with a specimen preparation punching machine (CEAST) shortly after the hot moulding process. The specimens were then stored at room temperature for one week

Preprints (www.preprints.org) | NOT PEER-REVIEWED | Posted: 15 March 2021 doi:10.20944/preprints202103.0361.v1

prior to testing in order to provide realistic industrial storage conditions of the processed material. Uniaxial tensile tests according to the ISO 527 standard were performed on a universal testing machine (SUN 2500, GALDABINI) at room temperature and a constant crosshead speed of 10 mm/min. The machine was equipped with a video extensometer (OS-65D CCD, Minstron). Tensile modulus is measured in the linear regime up the deformation of 1 %. The tensile strength is calculated as the maximum stress reached after the elastic regime and directly read from the engineering strain-stress curve. The strain at break is measured by direct read from the engineering strain-stress curve and the energy at break is calculated as the area under the engineering stress-strain curve until failure.

2.8. Impact-tensile tests

Impact tensile tests have been performed using a swinging pendulum (CEAST 6545, Torino, Italy) having a length L= 374 mm, assembled with a hammer having a mass of 3.655 kg and a potential energy of 25 J, is released from an angle of 45° and hits the specimen at its lower position with an impact energy of 3.93 J and an impact velocity of 1.47 m/s. The specimen, clamped with a crosshead of 60 g, is submitted to a high-speed tensile load. The tensile-impact strength a_{tU}, defined as the energy absorbed by the specimen until the fracture divided by the initial cross section $A_0 = t * b$, with t the thickness and b the width of the sample, has been determined through tensile-impact testing according to the standard ISO 8256. The same type of specimens as for tensile testing has been used (type 1BA), and the tests have been performed two weeks after the processing of the sheets.

3. Results

3.1. Ground Tire Rubber (GTR) properties

Prior to the mechanical characterization of the PLA/GTR blends, the properties of the GTR particles were studied. At a macro-scale, their size distribution, degradation properties and their chemical composition (**Figures 1-2**) were estimated. At the chains network scale, the average density and the distribution of the chains network depending on the applied grinding process and sieving mesh sizes (**Figure 3**) were determined.

The GTR particle size distribution was drastically reduced after sieving with the largest mesh (**Figure 1a**). As cryo-grinding usually results in smaller particle size as compared to ambient grinding [52], it was possible to sieve sufficient quantity of cryo-grinded GTR at higher mesh 230 ’s (size < 63 μm). The thermal stability of the sieved crumb GTR obtained from ambient and cryo-grinding processes is discussed based on TGA curves (**Figure 1b-c**). For all GTR, the first derivative peak around 360-380 °C is ascribed to the degradation of Natural Rubber, the second one situated around 420-445 °C to the degradation of SBR [53]. The remaining mass above 500 °C is ascribed to non-rubber components, that are mostly composed by carbon black (CB) particles. The degradation temperature of NR and SBR seems to not drastically depend on the nature of the grinding nor on the sieving. However, the fraction of non-rubber components is found to largely increase by decreasing the GTR size. This is possibly due to a gravity effect arising from the sieving process, as the fine and heavy non-rubber components, free or attached to the finest GTR particles, preferentially go through the sieves.

Preprints (www.preprints.org) | NOT PEER-REVIEWED | Posted: 15 March 2021 doi:10.20944/preprints202103.0361.v1

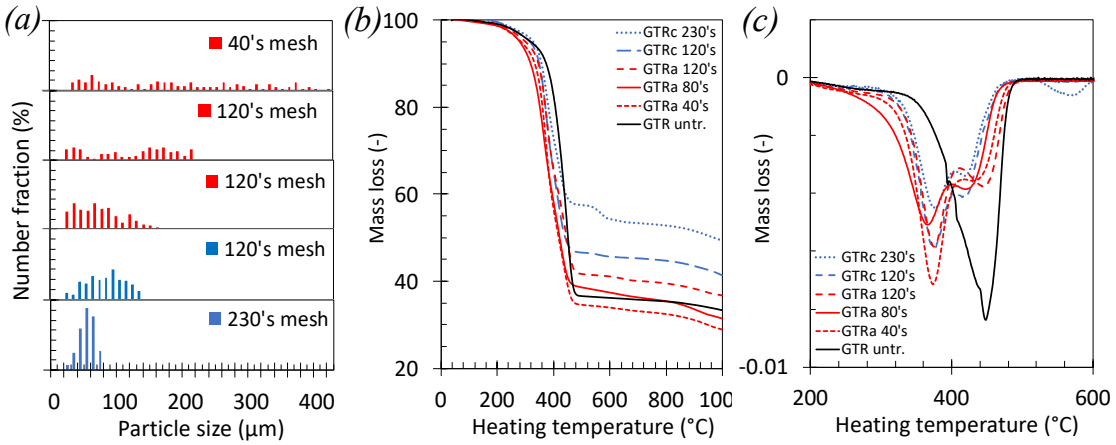

Figure 1. *(a)* Size distribution of dry ambient grinding and cryo-grinding of GTR particles, *(b)* Mass loss versus heating temperature obtained from TGA measurements and *(c)* first derivative of the mass loss versus heating temperature.

Grinding processes generally require clay minerals. Their presence is indeed shown by the preponderance of Magnesium (Mg) atoms as observed by EDX for highly sieved GTR$_c$ (**Figure 2**). The sulfur arising from the vulcanization (curing) of the tire is also present in the GTR. The ratio of Magnesium (Mg) over Sulphur (S) obtained from the quantitative EDX analysis of chemical elements is found to increase of 60% from the GTR$_c$ 120's mesh to GTR$_c$ 230's mesh, confirming the clay particles to be more present into sieved particles obtained with highest sieving mesh (finest size). The presence of these non-rubber components may explain the small TGA derivative peak close to 600 °C (**Figure 1c**) observed for the finest GTR$_c$ particles. At such high temperature, minerals like clay [54] or Kaolin [55] indeed start to decompose. In the following, the estimation of the network chain density of the GTR will be corrected from the presence of these non-rubber components, namely carbon black particles and clay minerals (**Figure 3**).

Preprints (www.preprints.org) | NOT PEER-REVIEWED | Posted: 15 March 2021 doi:10.20944/preprints202103.0361.v1

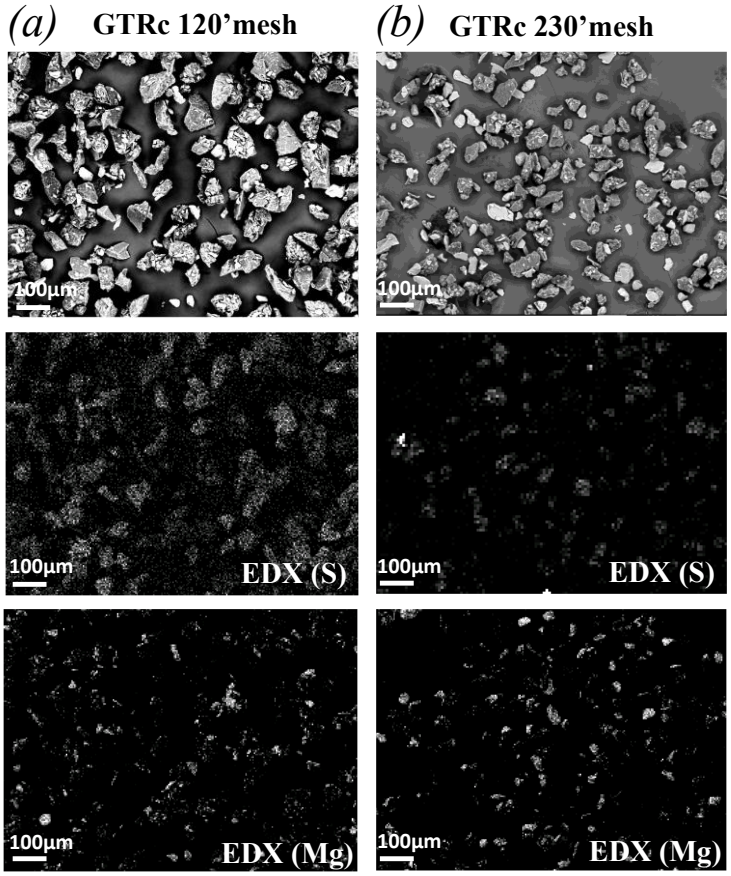

Figure 2. SEM images of GTR_c particles with 120's mesh *(a)* and 230's mesh sieving *(b)* at a magnitude X100 (top figures). Mapping of the sulphur contained into the GTR particles (center figures) and mapping of the Mg (bottom figures) obtained from chemical analysis by EDX.

The ground tire rubber crumbs produced by dry ambient and cryo-grinding of the used tire buffing were swollen into cyclohexane and the average network chain density and its distribution analysed (**Figure 3a-c**). GTR showed an overall increase of the swelling ratio, *Q*, from un-grinded (Q~ 1/0.45) to grinded GTRa (Q~ 1/0.25) and GTRc (Q~ 1/0.35). The lower swelling ratio of GTR_c as compared to GTR_a is likely explained by an increasing amount of non-rubber components in GTR_c, mostly carbon black (CB), as suggested by the TGA (**Figure 1b-c)**. After correction form the presence of non-rubber components, and assuming no adhesion between these rigid particles and the swollen rubber, the rubber network chains density has been calculated from the swelling ratio and using the Flory-Rehner equation (**Equ. 1-2**). The network chains density was found close to 1×10^{-4} $mol.cm^{-3}$ for all grinded GTR, independently on the size and on the grinding type (**Figure 3b**). These values are found much lower that the network chain density of the ungrinded GTR, found around 5.9×10^{-4} $mol.cm^{-3}$. This suggests the different tested grinding processes to show similar ability to damage the chains network and that the finest GTR size does not result from more intense damage. At molecular scale, such damage may traduce the rubber chains scission, sulphur-bonds breakage or rubber-filler rupture (**Figure 3b**). Possibly, the filler aggregates present into the GTR may also undergo filler-filler rupture, as had been discussed in the case of mechanically damaged carbon black filled rubbers [56],[57],[58].

Thermoporosimetry experiment is further used to reveal the distribution of the distance between the nodes of the rubber chains network (crosslinks or entanglements) of the GTR (**Figure 3c**). This method has been widely used in the case of bulk vulcanized rubber [59],[60]. It is applied here in the case of ground tire rubber particles. Thermoporosimetry is based on the quantification of the distribution of the melting temperature of

Preprints (www.preprints.org) | NOT PEER-REVIEWED | Posted: 15 March 2021 doi:10.20944/preprints202103.0361.v1

a crystallized rubber solvent trapped into the rubber network. Then, through the use of the Gibbs-Thomson equation (**Equ. 3-4**), the distribution of the crystallite sizes is calculated. Assuming these crystallites to be constrained by the network nodes (trapped physical entanglements or chemical crosslink), the distribution of the melting temperature directly relates to the distribution of the distance between the nodes (crosslinks or trapped entanglements). This distance is defined as the pores size. As indicated in **Figure 3c**, the shift of the average pore size to higher values as well as the increased distribution from un-grinded to grinded GTR is the result of more intense but heterogeneous damage of the chains network due to the mechanical cutting. Consistent with measures of the network chain density (**Figure 3a-b**), the pore size distribution is found very similar in all grinded GTR. In the following, it will be admitted that all sieved GTR exhibit similar average network chains densities with rather broad distribution. Such properties are found independent on the size and grinding type. The level of damage in the network chain density of the GTR as well as their non-rubber content are expected to have both a role in the tensile behaviour of the PLA/GTR blends, as will be discussed in the subsequent sections.

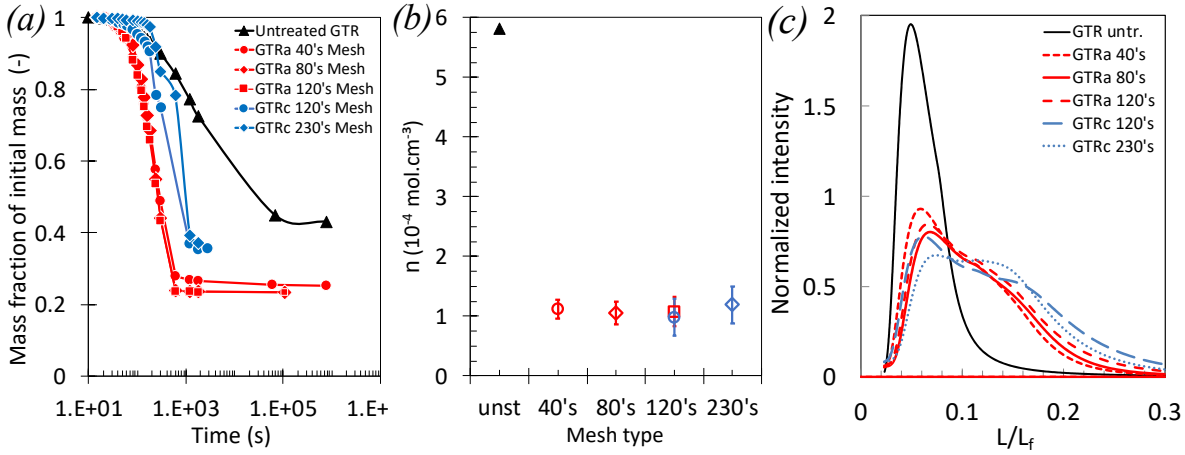

Figure 3. *(a)* deswelling kinetics in swollen grinded GTR crumbs of different sizes displayed by mass fraction of the initial mass versus logarithmic time. *(b)* network chains densities of grinded GTR crumbs of different particle sizes whose mesh types are detailed in the experimental section. *(c)* Normalized intensity versus normalized pores size of grinded GTR crumbs of different particle sizes extracted from thermoporosimetry experiments (see experimental section for more details on the procedure).

3.2. Tensile properties of PLA/GTR blends: Effect of the GTR size

PLA/GTRa and PLA/GTRc blends using 15 wt.% of sieved dry ambient grinded GTRa and sieved cryo-grinded GTRc were processed and their tensile properties presented (Figures 4-5). While the swelling methods cannot indicate the percentage of chains scission or sulphur bond breakage occurring during grinding, the low network chain density of the GTR (Figure 3b), resulting from the mechanical cutting is expected to, at least partially, result from devulcanization (sulphur bond breakage). GTR treated by grinding is indeed expected to possess a certain reactivity and a possible re-vulcanization can be envisaged [61]. To this aim, the effect of a curing agent (DCP) has been investigated in the case of PLA/GTRa blends. One may note that the effect of DCP has also been investigated for PLA/GTRa blends, on a selection of the finest GTRc particles and for a unique GTRc content of 15 wt.% (see section 3.3).

Stress strain tensile curve of neat PLA shows linearity up to 2% of deformation followed by a yielding at around 3%. No post-yielding deformation is noted as the PLA rapidly breaks at 3.5% (**Figure 4**). This brittle behaviour of PLA is due to the storage at ambient temperature sufficiently long to cause a ductile to brittle transition due to physical aging [62]. The addition of 15 wt.% of GTR results in a decreased yield strength, arising from rubber particles softening and likely voids formation at PLA/GTR interface.

Preprints (www.preprints.org) | NOT PEER-REVIEWED | Posted: 15 March 2021 doi:10.20944/preprints202103.0361.v1

However, a plastic plateau is observed, indicating the PLA/GTR blends to be more ductile as compared to neat PLA.

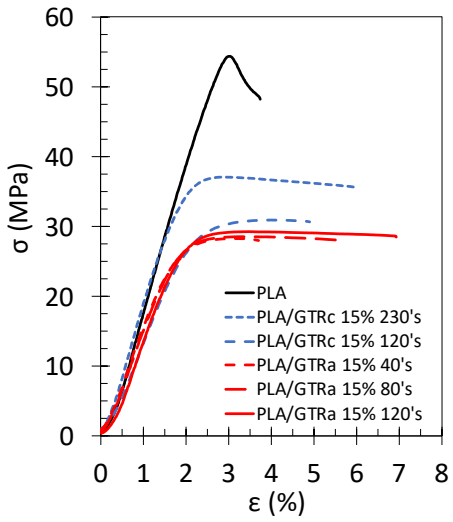

Figure 4. Engineering stress-strain curves of tensile test performed at 10 mm.min^{-1} and at room temperature on the neat PLA (black continuous line), PLA/GTR$_a$ 15 wt.% sieved 40's mesh (red dashed dotted line), PLA/GTR$_a$ 15 wt.% sieved 80's mesh (red dotted line), PLA/GTR$_a$ 15 wt.% sieved 120's mesh (red continuous line), PLA/GTR$_c$ 15 wt.% sieved 120's mesh (blue large dotted line) and PLA/GTR$_a$ 15 wt.% sieved 200's mesh (blue small dotted line). Tensile curves shown in this study correspond to PLA/GTR blends using DCP at 1.5 wt.% of the GTR. The effect of DCP content is further detailed in **Figure 5**.

In all PLA/GTR blends, the stiffness and strength are found lower that the ones of the neat PLA, expectedly due to the introduction of rubbery particles into the glassy PLA matrix. The elastic modulus and yield strength in PLA/GTR$_a$ seem weakly dependent on the particle sizes (**Figure 5a-b**). However, the elastic modulus of the neat PLA is recovered for the PLA/GTR$_c$ blends incorporating the finest GTR$_c$. The strength is also increased consistent with previously reported results in TPE using wastes rubber in the same range of sizes [24]. This notable rise in stiffness and strength with lowering the GTR sizes may additionally find origin in the presence of significant non-rubber fraction in the finest GTR$_c$ (more than 50 wt. % from TGA, **Figure 1b**), mostly composed by carbon black particles, that contribute to mechanically reinforce the GTR and by inference the PLA/GTR blend. Moreover, the micron sized clay particles used in cryo-grinding process (**Figure 2b-c**) – possibly dispersed into the PLA during melt-blend with GTR – have been demonstrated to also mechanically reinforce the PLA matrix [63],[64].

The strain and energy at break both show visible increase when incorporating finer GTR, independently on the type of grinding (**Figure 5c-d**). A homogeneous particle distribution into the PLA matrix is suggested by SEM images (**Figure 10**, **Figure S1**. Hence, the wider number of distributed and fine GTR particles distributes the stress upon loading and may result in cavitation/decohesion at PLA/GTR rather than in brittle failure through the development of crazes as usually the case in the neat brittle PLA [22],[24].

The addition of the vulcanizing agent, DCP, is found to result in a perceptible increase of the strain and energy at break. This effect is more pronounced in blends using the finest GTR particles. DCP had been demonstrated to be an efficient crosslinking agent for PLA and natural rubber (NR) [12],[13],[46]. The presence of DCP to form free radical may crosslink both PLA and GTR particles, as they are assumed to be partially devulcanized regarding their low network chains density (**Figure 3b**). The action of free radicals at PLA/GTR interface is expected to be more efficient for the finest GTR as their containing more potential crosslinking sites due to their large surface area.

Preprints (www.preprints.org) | NOT PEER-REVIEWED | Posted: 15 March 2021 doi:10.20944/preprints202103.0361.v1

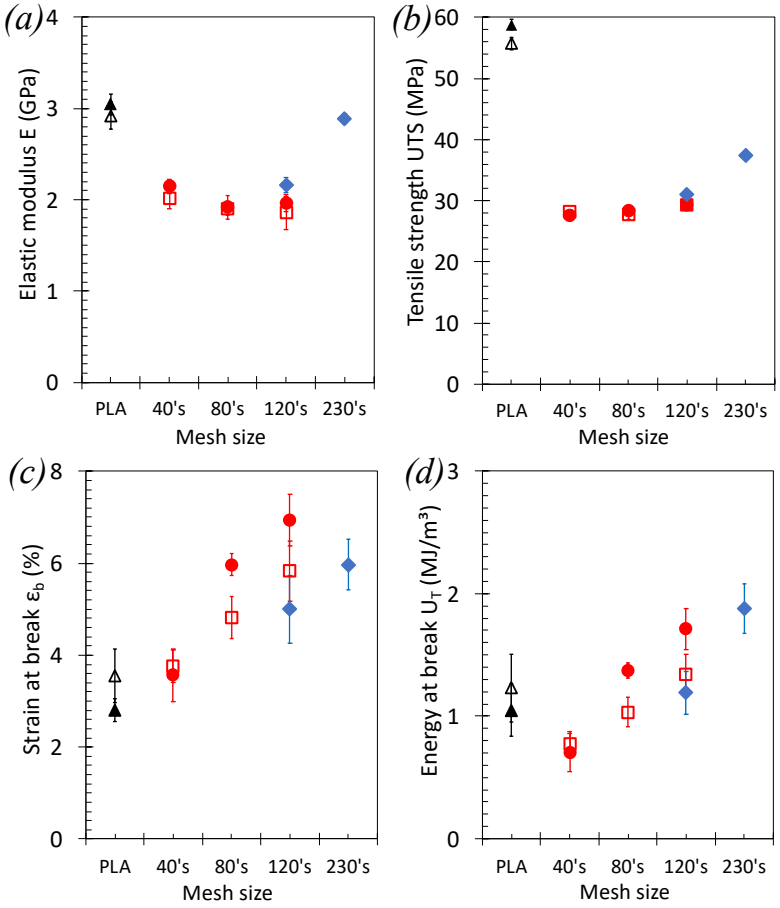

Figure 5. Effect of the GTR size on the tensile properties of PLA/GTR blends. *(a)* elastic modulus, E_T, *(b)* tensile strength UTS, *(c)* strain at break, ε_b, and *(d)* energy at break, U_T, measured from tensile test performed at 10 mm.min^{-1} and at room temperature: neat PLA in absence of DCP (black unfilled triangle symbols), neat PLA in presence of 1.5 wt.% DCP (black filled triangle symbols), PLA/GTR$_a$ 15% in absence of DCP (red square symbols), PLA/GTR$_a$ 15% in presence of 1.5 wt.% of DCP (red ring symbols) and PLA/GTR$_c$ 15% in presence of 1.5 wt.% of DCP (blue diamond symbols). All blends were processed at 170 °C in presence of Irganox (0.2 wt.% of total amount of material).

3.3. Tensile properties of PLA-GTR blends: effect of the GTR content

The effect of the GTR content, from 0 to 30 wt.% has been studied using the PLA/GTR$_a$ blends containing the finest GTR$_a$ 120's mesh (**Figure 6-7**). The increasing amount of GTR results in a decreased strength, arising from rubber particles softening. For all rubber content and in presence of crosslinking agent or not, stress strain tensile curves of the PLA-GTR$_a$ blends (**Figure 6**) show more ductile behaviour with a larger plastic plateau as compared to the brittle behaviour of neat PLA, as previously discussed (**Figure 4**).

Preprints (www.preprints.org) | NOT PEER-REVIEWED | Posted: 15 March 2021 doi:10.20944/preprints202103.0361.v1

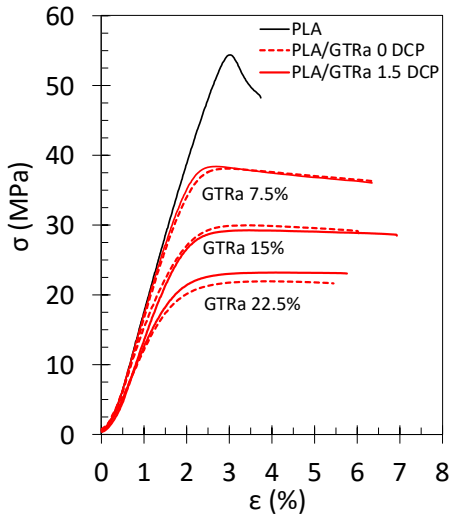

Figure 6. Engineering stress-strain curves of tensile test performed at 10 mm.min^{-1} and at room temperature on the neat PLA without DCP (black continuous line), PLA/GTR$_a$ 7.5, 15 and 22.5% sieved 120's mesh without DCP (red dotted lines) and PLA/GTR$_a$ 7.5, 15 and 22.5% sieved 120's mesh with 1.5 wt.% DCP (red continuous line). All blends were processed at 170 °C in presence of Irganox (0.2 wt.% of total amount of material).

The increasing amount of rubber particles results in a drop in tensile modulus, E_T, and tensile strength, *UTS*, of the PLA/GTR$_a$ blends (**Figure 7a-b**). The introduction of DCP has beneficial effect on the elastic modulus. This effect is more pronounced with an increased amount of GTR and may results in (i) crosslinking of the PLA matrix as suggested in Ref. [65], (ii) re-crosslinking of the GTR, (iii) co-crosslinking at PLA/GTR interface that all potentially participate in the increased stiffness of the PLA/GTR blend.

By increasing the GTR content from 0 to 22.5 wt. %, the strain and energy at break increase to reach a maximum at an optimum quantity of GTR between 7.5 and 15 wt. % (**Figure 7c-d**). However, a drastic decrease of strain and energy at break above this optimum may be caused by an agglomeration of the rubber particles. The DCP is beneficial to the strain and energy at break in the PLA/GTR$_a$ blends for a content at and above 15 wt.%. Hence, in spite of the expected decreased ductility of the PLA matrix due to DCP crosslinking of the neat PLA ([65], see also **Figure 5c-d**), the visible increased ductility of the PLA/GTR blend suggests the beneficial role of the reinforcement of the PLA/GTR interface via a possible co-crosslinking of rubber and PLA chains, as had previously been demonstrated in PLA/NR blends [34],[35].

Preprints (www.preprints.org) | NOT PEER-REVIEWED | Posted: 15 March 2021 doi:10.20944/preprints202103.0361.v1

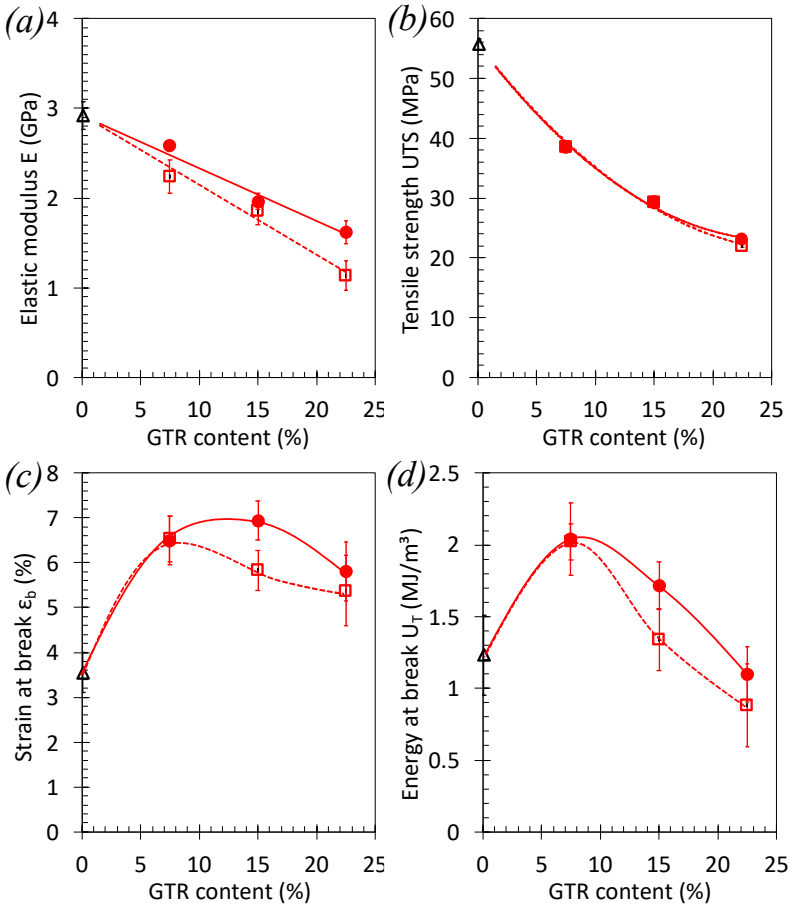

Figure 7. Effect of the GTR content on the tensile properties of PLA/GTR blends. *(a)* elastic modulus, E_T, *(b)* tensile strength UTS, *(c)* strain at break, ε_b, and *(d)* energy at break, U_T, from tensile test performed at 10 mm.min^{-1} and at room temperature on the neat PLA in absence of DCP (black triangle symbols), PLA/GTR$_a$ in absence of DCP (red unfilled square symbols) and in presence of 1.5 wt.% of DCP (red filled circle symbols). All blends were processed at 170 °C in presence of Irganox (0.2 wt.% of total amount of material).

The effect of the GTR particle content, from 0 to 30 wt.% has been studied for the blends containing the finest GTR$_c$ particles, namely PLA/GTR$_c$ 230's (**Figure 8-9**). The addition of increasing amount of GTR, results in a decreased strength, but to a lower extent as compared to blends using GTR$_a$ (**Figure 6-7**). Stress strain tensile curves of the PLA-GTR blends (**Figure 8**) show more ductile behaviour with a larger plastic plateau as compared to the brittle behaviour of neat PLA.

Preprints (www.preprints.org) | NOT PEER-REVIEWED | Posted: 15 March 2021 doi:10.20944/preprints202103.0361.v1

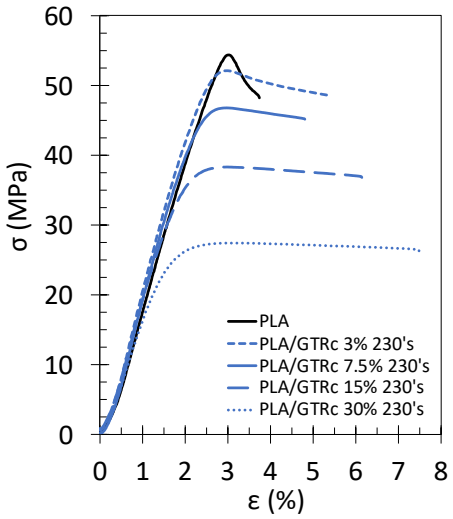

Figure 8. Engineering stress-strain curves of tensile test performed at 10 mm.min^{-1} and at room temperature on the neat PLA without DCP (black continuous line), PLA/GTR$_a$ 7.5, 15 and 30 wt.% sieved 230's mesh with 1.5 wt.% DCP (blue lines). All blends were processed at 170 °C in presence of Irganox (0.2 wt.% of total amount of material).

Interestingly, the introduction of GTR particles at low amount (3 wt.%) results in an increase of tensile modulus, E_T, and only small drop in tensile strength of the PLA/GTR$_c$ blends (**Figure 9a-b**). Above this content, a decrease of the elastic modulus and tensile strength is observed, but much lower as compared to PLA/GTR$_a$ (**Figure 7a-b**). These results are likely explained by (i) the finer rubber particles extracted from cryo-grinding and (ii) the higher quantity of non-rubber reinforcing elements in blends using finest cryo-grinded GTR, sized clay (**Figure 1a-b)**.

By increasing the GTR content up to 30 wt. %, the strain and energy at break increase with the quantity of GTR introduced (**Figure 9c-d**). The maintain of higher values of strain and energy at break as compared to the one of neat PLA and to the PLA/ GTR$_a$ blends ((**Figure 7c-d**) is allowed by the fine GTR size, expected to be well dispersed into the PLA matrix (see SEM images on **Figure 10**). The influence of the crosslinking agent is evidenced here in PLA/GTR$_c$ 15% blends as it results in a mutual increase of the elastic modulus, strain at break and energy at break (**Figure 9a-d**). This result is consistent with a possible reinforcement of the PLA/GTR interface via co-crosslinking of the GTR and PLA, while a simple crosslinking of the PLA matrix and/or GTR particles would have resulted in a stiffer but less deformable blends.

Preprints (www.preprints.org) | NOT PEER-REVIEWED | Posted: 15 March 2021 doi:10.20944/preprints202103.0361.v1

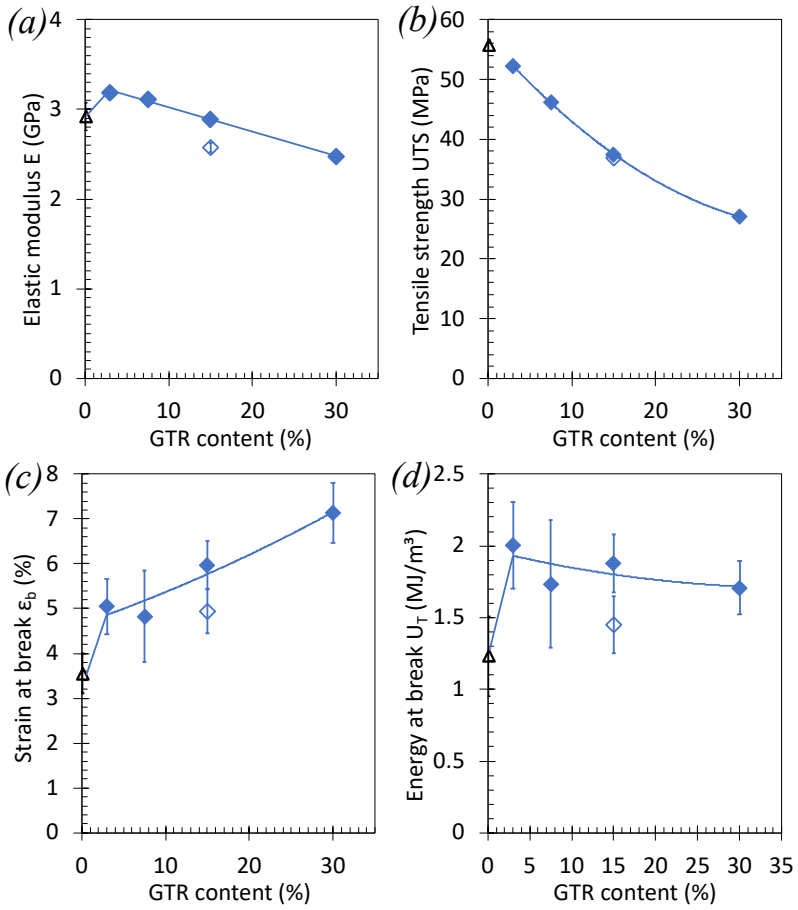

Figure 9. Effect of the GTR content on the tensile properties of PLA/GTR blends. *(a)* elastic modulus, E_T, *(b)* yield strength σ_y, *(c)* strain at break, ε_b, and *(d)* energy at break, U_T, from tensile test performed at 10 mm.min^{-1} and at room temperature on the neat PLA (black triangle symbols), PLA/GTR$_c$ in presence of 1.5 wt.% of DCP (blue diamond symbols). All blends were processed at 170 °C in presence of Irganox (0.2 wt.% of total amount of material).

The fracture surface at cross-section of the mechanically tested PLA and PLA-GTR were analysed by SEM (**Figure 10, Figure S1**). The deformation mechanism of the brittle PLA had been demonstrated to result in the formation of surface crazes [66], resulting in a smooth fracture surface (**Figure 10a-b**). PLA/GTR$_a$ and PLA/GTR$_c$ blends with GTR up to 15 wt.%, the micrographs show a relatively homogeneous dispersion of the GTR particles in the PLA matrix (**Figure 10c-h**). This is confirmed by EDX images as attested by the sulphur-rich domains indicating the presence of the GTR particles (**Figure S1**). Moreover, SEM micrographs reveal a good adhesion of some of the GTR particles to the PLA matrix (**Figure 10c-h**) while some other show partial decohesion, resulting from damage occurring during tensile test. As previously commented, these damage mechanisms may reduce the stress concentration at PLA/GTR interface and results in a larger plastic deformation that in neat PLA (**Figure 6**, **Figure 8**). However, their maintain up to the largest deformation possible should result in delayed macroscopic failure, which would be facilitated for instance by the presence of the DCP agent participating in a possible co-cross-linking at PLA/GTR interface as previously discussed.

Preprints (www.preprints.org) | NOT PEER-REVIEWED | Posted: 15 March 2021 doi:10.20944/preprints202103.0361.v1

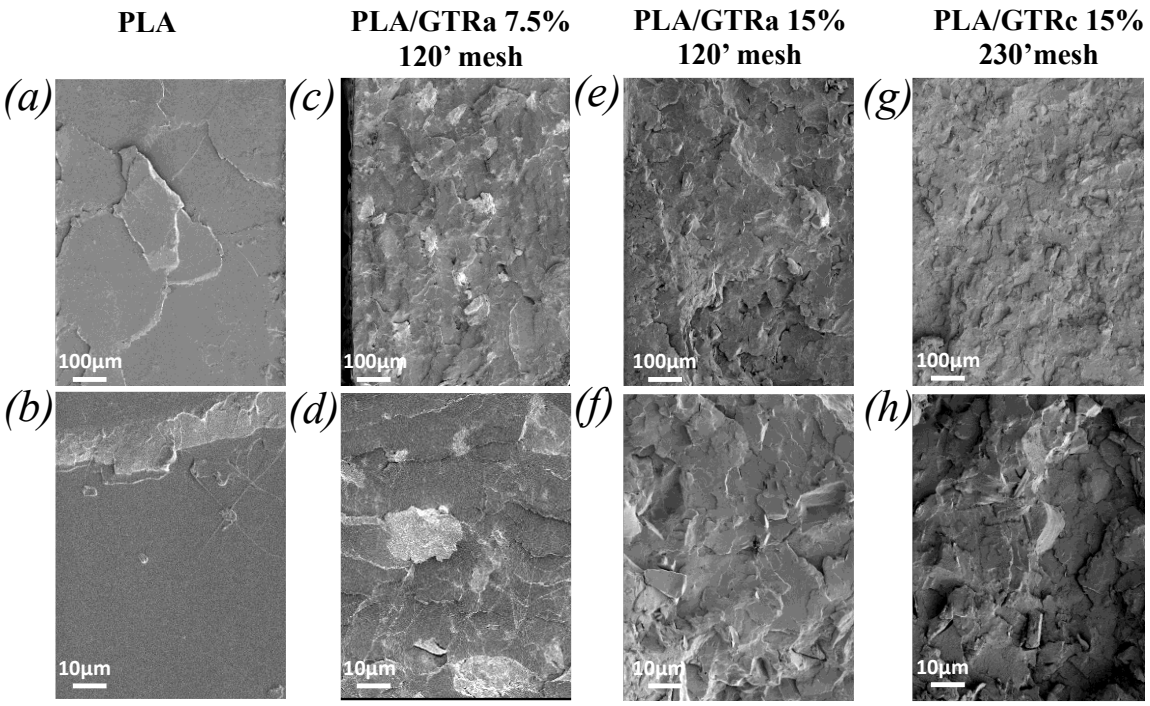

Figure 10. SEM images of fracture surface at two magnitudes x 100 (top) and x 1000 (bottom) of neat PLA (a-b), PLA/GTR$_a$ 7.5 wt.% (c-d) with DCP, PLA/GTR$_a$ 15 wt.% (c-d) with DCP, PLA/GTR$_c$ 7.5 wt.% (c-d) with DCP, PLA/GTR$_a$ 15 wt.% (c-d) with DCP.

The materials showing the most promising mechanical performance measured during tensile test, namely PLA/GTR$_c$ with 230's mesh sized GTR particles (**Figure 8-9**), had then been subjected to tensile impact. Consistent with increased tensile energy at break of the PLA/GTR blends as compared to the more brittle PLA (**Figure 9d**), tensile impact strength also increases in the PLA/GTR blends (**Figure 11**). Moreover, a substantial increase (1-fold) of the impact strength of crosslinked PLA/GTR 15% is found as compared to un-crosslinked PLA/GTR 15%, highlighting the role of co-crosslinking at PLA/GTR interface to prevent macroscopic failure in impact conditions (high strain loading). Crosslinked PLA/GTR blends using 15% of fine cryo-grinded GTR comply with the requirements for a sustainable route for wastes rubber recycling. Moreover, they represent a reasonable compromise in terms of mechanical performance. In spite of a 30% drop of the PLA tensile strength, the elastic modulus of PLA is maintained, the strain at break is increased of 80%, the energy at break is increased of 60% and the impact strength is increased of 90%.

Preprints (www.preprints.org) | NOT PEER-REVIEWED | Posted: 15 March 2021 doi:10.20944/preprints202103.0361.v1

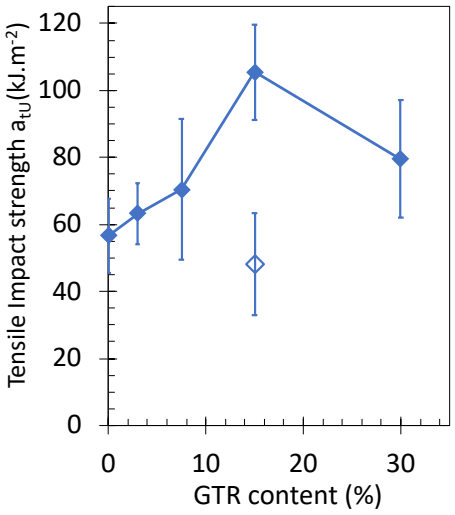

Figure 11. Tensile impact strength of neat PLA and PLA/GTR$_c$ blends in presence of 1.5 wt.% of DCP (filled diamond symbols). PLA/GTR$_c$ containing 15 wt.% of GTR in absence of DCP is added as a reference material (unfilled diamond symbols). All blends were processed at 170 °C in presence of Irganox (0.2 wt.% of total amount of material).

4. Conclusion

PLA/GTR blends using crosslinking agent were prepared as a route to recycle wastes rubber from the automotive industry (GTR) and improve the toughness of the bio-based brittle PLA. Firstly, the physico-chemical properties of the GTR were investigated, secondly the tensile and impact properties of the PLA/GTR blends were presented.

It has been found that the grinding of the GTR resulted in a wide mechanical damage of the rubber network as attested by a large decrease of their chains network density which may have resulted from chains scission (reclaiming) and sulphur-bonds breakage (devulcanization). The GTR particles treated by grinding are hence expected to possess a certain reactivity prone to a further re-vulcanization. Moreover, it has been found that the finest sieved GTR particles were accompanied by the largest the amount of non-rubber reinforcing components (carbon black particles, clay).

Based on the prior GTR characterization, PLA/GTR blends have been processed by using DCP as a mutual crosslinking agent of GTR and PLA. The use of the finest cryo-grinded in the presence of DCP as co-crosslinking agent, showed the least decrease of the tensile strength (-30%), a maintain of the tensile modulus and the largest improvement of the strain at break (+80%), energy at break (+60%) and impact strength (+90%) as compared to the neat PLA. The results were attributed to several factors: the good dispersion of the fine GTR particles into the PLA matrix, the partial re-crosslinking of the GTR particles and co-crosslinking at PLA/GTR interface and the presence of reinforcing carbon black into the GTR particles and clay particles dispersed into the PLA matrix.

Author Contributions: For research articles with several authors, a short paragraph specifying their individual contributions must be provided. The following statements should be used "Conceptualization, N. Candau.; methodology, N. Candau., Noel León Albiter., Gero Förster; software, N. Candau; formal analysis, N. Candau.; investigation, N. Candau., Oguzhan Oguz., Gero Förster; Noel León Albiter., data curation, N. Candau., Noel León Albiter., Gero Förster; writing—original draft preparation, N. Candau.; writing—review and editing, N. Candau., Oguzhan Oguz., supervision, María Lluïsa Maspoch.; project administration, María Lluïsa Maspoch., funding acquisition, María Lluïsa Maspoch. All authors have read and agreed to the published version of the manuscript."

Funding: The research leading to these results have received funding from the People Program (Marie Curie Actions) under grant agreement no. 712949 (Tecniospring Plus Program) and from the Agency for Business Competitiveness of the Government of Catalonia ACCIÓ.

 doi:10.20944/preprints202103.0361.v1

Acknowledgments: The research leading to these results has received funding from the European Union's Horizon 2020 research and innovation programme under the Marie Skłodowska-Curie grant agreement No 712949 (TECNIOspring PLUS) and from the Agency for Business Competitiveness of the Government of Catalonia.

Conflicts of Interest: The authors declare no conflict of interest. The funders had no role in the design of the study; in the collection, analyses, or interpretation of data; in the writing of the manuscript, or in the decision to publish the results.

Appendix

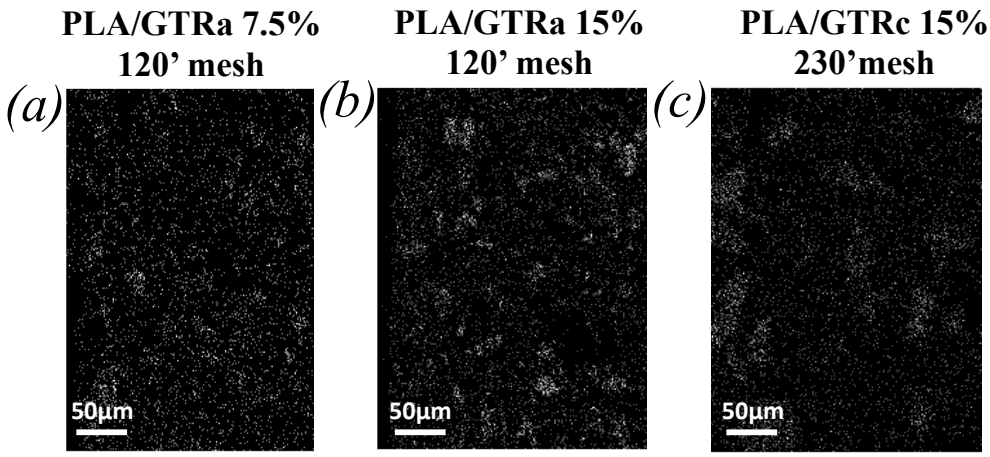

Figure S1. SEM-EDX images of fracture surface at two magnitudes x 100 (top) and x 1000 (bottom) of neat PLA (a-b), PLA/GTR$_a$ 7.5 wt.% (c-d) with DCP, PLA/GTR$_a$ 15 wt.% (c-d) with DCP, PLA/GTR$_c$ 7.5 wt.% (c-d) with DCP, PLA/GTR$_a$ 15 wt.% (c-d) with DCP.

References

[1] European Commission, « A European Strategy for Plastics in a Circular Economy », 2018. .

[2] B. Adhikari, D. De, et S. Maiti, « Reclamation and recycling of waste rubber », *Prog. Polym. Sci.*, vol. 25, nº 7, p. 909-948, sept. 2000, doi: 10.1016/S0079-6700(00)00020-4.

[3] M. Sienkiewicz, H. Janik, K. Borzędowska-Labuda, et J. Kucińska-Lipka, « Environmentally friendly polymer-rubber composites obtained from waste tyres: A review », *J. Clean. Prod.*, vol. 147, p. 560-571, mars 2017, doi: 10.1016/j.jclepro.2017.01.121.

[4] S. Spierling *et al.*, « Bio-based plastics - A review of environmental, social and economic impact assessments », *J. Clean. Prod.*, vol. 185, p. 476-491, juin 2018, doi: 10.1016/j.jclepro.2018.03.014.

[5] T. Iwata, « Biodegradable and Bio-Based Polymers: Future Prospects of Eco-Friendly Plastics », *Angew. Chem. Int. Ed.*, vol. 54, nº 11, p. 3210-3215, 2015, doi: https://doi.org/10.1002/anie.201410770.

[6] Y. Ikeda, A. Kato, S. Kohjiya, et Y. Nakajima, *Rubber Science: A Modern Approach*. Springer Singapore, 2018.

[7] Y. Kikuchi, T. Fukui, T. Okada, et T. Inoue, « Elastic-plastic analysis of the deformation mechanism of PP-EPDM thermoplastic elastomer: Origin of rubber elasticity », *Polym. Eng. Sci.*, vol. 31, nº 14, p. 1029-1032, 1991, doi: 10.1002/pen.760311406.

[8] S. Abdou-Sabet, R. C. Puydak, et C. P. Rader, « Dynamically Vulcanized Thermoplastic Elastomers », *Rubber Chem. Technol.*, vol. 69, nº 3, p. 476-494, juill. 1996, doi: 10.5254/1.3538382.

[9] V. Tanrattanakul, K. Kosonmetee, et P. Laokijcharoen, « Polypropylene/natural rubber thermoplastic elastomer: Effect of phenolic resin as a vulcanizing agent on mechanical properties and morphology », *J. Appl. Polym. Sci.*, vol. 112, nº 6, p. 3267-3275, juin 2009, doi: 10.1002/app.29816.

[10] C. Nakason, S. Jamjinno, A. Kaesaman, et S. Kiatkamjornwong, « Thermoplastic elastomer based on high-density polyethylene/natural rubber blends: rheological, thermal, and morphological properties », *Polym. Adv. Technol.*, vol. 19, nº 2, p. 85-98, 2008, doi: 10.1002/pat.972.

[11] O. Oguz, N. Candau, M. K. Citak, F. N. Cetin, S. Avaz Seven, et Y. Z. Menceloglu, « A Sustainable Approach to Produce Stiff, Super-Tough, and Heat-Resistant Poly(lactic acid)-Based Green Materials », *ACS Sustain. Chem. Eng.*, vol. 7, nº 8, p. 7869-7877, avr. 2019, doi: 10.1021/acssuschemeng.9b00319.

[12] D.-D. Yang, C. Wu, G. Wu, S.-C. Chen, et Y.-Z. Wang, « Toughening of Polylactide with High Tensile Strength via Constructing an Integrative Physical Crosslinking Network Based on Ionic Interactions », *Macromolecules*, déc. 2020, doi: 10.1021/acs.macromol.0c02181.

[13] D. Yuan, Z. Chen, C. Xu, K. Chen, et Y. Chen, « Fully Biobased Shape Memory Material Based on Novel Cocontinuous Structure in Poly(Lactic Acid)/Natural Rubber TPVs Fabricated via Peroxide-Induced Dynamic Vulcanization and in Situ Interfacial Compatibilization », *ACS Sustain. Chem. Eng.*, vol. 3, nº 11, p. 2856-2865, nov. 2015, doi: 10.1021/acssuschemeng.5b00788.

[14] X. Zhang, C. Lu, et M. Liang, « Preparation of thermoplastic vulcanizates based on waste crosslinked polyethylene and ground tire rubber through dynamic vulcanization », *J. Appl. Polym. Sci.*, vol. 122, nº 3, p. 2110-2120, 2011, doi: https://doi.org/10.1002/app.34293.

[15] P. Nevatia, T. S. Banerjee, B. Dutta, A. Jha, A. K. Naskar, et A. K. Bhowmick, « Thermoplastic elastomers from reclaimed rubber and waste plastics », *J. Appl. Polym. Sci.*, vol. 83, nº 9, p. 2035-2042, 2002, doi: https://doi.org/10.1002/app.10115.

[16] C. Radheshkumar et J. Karger-Kocsis, « Thermoplastic dynamic vulcanisates containing LDPE, rubber, and thermochemically reclaimed ground tyre rubber », *Plast. Rubber Compos.*, vol. 31, nº 3, p. 99-105, mars 2002, doi: 10.1179/146580102225003074.

[17] S. Al-Malaika et E. J. Amir, « Thermoplastic elastomers: Part III—Ageing and mechanical properties of natural rubber-reclaimed rubber/polypropylene systems and their role as solid phase dispersants in polypropylene/polyethylene blends », *Polym. Degrad. Stab.*, vol. 26, nº 1, p. 31-41, janv. 1989, doi: 10.1016/0141-3910(89)90026-8.

[18] X. Colom, J. Cañavate, F. Carrillo, et J. J. Suñol, « Effect of the particle size and acid pretreatments on compatibility and properties of recycled HDPE plastic bottles filled with ground tyre powder », *J. Appl. Polym. Sci.*, vol. 112, nº 4, p. 1882-1890, 2009, doi: https://doi.org/10.1002/app.29611.

[19] R. Sonnier, E. Leroy, L. Clerc, A. Bergeret, et J. M. Lopez-Cuesta, « Compatibilisation of polyethylene/ground tyre rubber blends by γ irradiation », *Polym. Degrad. Stab.*, vol. 91, nº 10, p. 2375-2379, oct. 2006, doi: 10.1016/j.polymdegradstab.2006.04.001.

[20] S. Tantayanon et S. Juikham, « Enhanced toughening of poly(propylene) with reclaimed-tire rubber », *J. Appl. Polym. Sci.*, vol. 91, nº 1, p. 510-515, 2004, doi: https://doi.org/10.1002/app.13182.

[21] R. Mujal-Rosas, J. Orrit-Prat, X. Ramis-Juan, M. Marin-Genesca, et A. Rahhali, « Study on dielectric, thermal, and mechanical properties of the ethylene vinyl acetate reinforced with ground tire rubber », *J. Reinf. Plast. Compos.*, vol. 30, nº 7, p. 581-592, avr. 2011, doi: 10.1177/0731684411399135.

[22] M. Awang, H. Ismail, et M. A. Hazizan, « Polypropylene-based blends containing waste tire dust: Effects of trans-polyoctylene rubber (TOR) and dynamic vulcanization », *Polym. Test.*, vol. 26, nº 6, p. 779-787, sept. 2007, doi: 10.1016/j.polymertesting.2007.04.007.

[23] P. Lima, J. Oliveira, et V. Costa, « Partial replacement of EPDM by GTR in thermoplastic elastomers based on PP/EPDM: Effects on morphology and mechanical properties », *J. Appl. Polym. Sci.*, vol. 131, nº 8, 2014, doi: 10.1002/app.40160.

[24] S. Ramarad, M. Khalid, C. T. Ratnam, A. L. Chuah, et W. Rashmi, « Waste tire rubber in polymer blends: A review on the evolution, properties and future », juill. 2015, doi: 10.1016/j.pmatsci.2015.02.004.

[25] C. L. Hel, V. Bounor-Legaré, M. Catherin, A. Lucas, A. Thèvenon, et P. Cassagnau, « TPV: A New Insight on the Rubber Morphology and Mechanic/Elastic Properties », *Polymers*, vol. 12, nº 10, p. 2315, oct. 2020, doi: 10.3390/polym12102315.

[26] R. Sonnier *et al.*, « Compatibilizing thermoplastic/ground tyre rubber powder blends: Efficiency and limits », *Polym. Test.*, vol. 27, nº 7, p. 901-907, oct. 2008, doi: 10.1016/j.polymertesting.2008.07.003.

[27] J. Cailloux *et al.*, « Melt-processing of cellulose nanofibril/polylactide bionanocomposites via a sustainable polyethylene glycol-based carrier system », *Carbohydr. Polym.*, vol. 224, p. 115188, nov. 2019, doi: 10.1016/j.carbpol.2019.115188.

[28] O. Oguz *et al.*, « Poly(lactide)/cellulose nanocrystal nanocomposites by high-shear mixing », *Polym. Eng. Sci.*, vol. n/a, nº n/a, doi: https://doi.org/10.1002/pen.25621.

[29] O. Oguz *et al.*, « High-Performance Green Composites of Poly(lactic acid) and Waste Cellulose Fibers Prepared by High-Shear Thermokinetic Mixing », *Ind. Eng. Chem. Res.*, vol. 56, nº 30, p. 8568-8579, août 2017, doi: 10.1021/acs.iecr.7b02037.

[30] P. Ma, D. G. Hristova-Bogaerds, J. G. P. Goossens, A. B. Spoelstra, Y. Zhang, et P. J. Lemstra, « Toughening of poly(lactic acid) by ethylene-co-vinyl acetate copolymer with different vinyl acetate contents », *Eur. Polym. J.*, vol. 48, nº 1, p. 146-154, janv. 2012, doi: 10.1016/j.eurpolymj.2011.10.015.

[31] J. Cailloux *et al.*, « Effect of the viscosity ratio on the PLA/PA10.10 bioblends morphology and mechanical properties », *Express Polym. Lett.*, vol. 12, nº 6, p. 569-582, janv. 2018, doi: 10.3144/expresspolymlett.2018.47.

[32] M. Harada, K. Iida, K. Okamoto, H. Hayashi, et K. Hirano, « Reactive compatibilization of biodegradable poly(lactic acid)/poly(ε-caprolactone) blends with reactive processing agents », *Polym. Eng. Sci.*, vol. 48, nº 7, p. 1359-1368, 2008, doi: https://doi.org/10.1002/pen.21088.

[33] Y. Feng, Y. Hu, J. Yin, G. Zhao, et W. Jiang, « High impact poly(lactic acid)/poly(ethylene octene) blends prepared by reactive blending », *Polym. Eng. Sci.*, vol. 53, nº 2, p. 389-396, 2013, doi: https://doi.org/10.1002/pen.23265.

[34] V. Nagarajan, A. K. Mohanty, et M. Misra, « Perspective on Polylactic Acid (PLA) based Sustainable Materials for Durable Applications: Focus on Toughness and Heat Resistance », *ACS Sustain. Chem. Eng.*, vol. 4, nº 6, p. 2899-2916, juin 2016, doi: 10.1021/acssuschemeng.6b00321.

[35] R. Wang, S. Wang, Y. Zhang, C. Wan, et P. Ma, « Toughening modification of PLLA/PBS blends via in situ compatibilization », *Polym. Eng. Sci.*, vol. 49, nº 1, p. 26-33, 2009, doi: 10.1002/pen.21210.

[36] Q. Zhao, Y. Ding, B. Yang, N. Ning, et Q. Fu, « Highly efficient toughening effect of ultrafine full-vulcanized powdered rubber on poly(lactic acid)(PLA) », *Polym. Test.*, vol. 32, nº 2, p. 299-305, avr. 2013, doi: 10.1016/j.polymertesting.2012.11.012.

[37] M. Oliveira, E. Santos, A. Araújo, G. J. M. Fechine, A. V. Machado, et G. Botelho, « The role of shear and stabilizer on PLA degradation », *Polym. Test.*, vol. 51, p. 109-116, mai 2016, doi: 10.1016/j.polymertesting.2016.03.005.

[38] S. Rabiei et A. Shojaei, « Vulcanization kinetics and reversion behavior of natural rubber/styrene-butadiene rubber blend filled with nanodiamond – the role of sulfur curing system », *Eur. Polym. J.*, vol. 81, p. 98-113, août 2016, doi: 10.1016/j.eurpolymj.2016.05.021.

[39] E. Leroy, A. Souid, et R. Deterre, « A continuous kinetic model of rubber vulcanization predicting induction and reversion », *Polym. Test.*, vol. 32, nº 3, p. 575-582, mai 2013, doi: 10.1016/j.polymertesting.2013.01.003.

[40] C. R. Rios-Soberanis, S. Wakayama, T. Sakai, J. de los Á. Rodriguez-Laviada, et E. Pérez-Pacheco, « Manufacture of Partially Biodegradable Composite Materials Based on PLA-Tires Powder: Process and Characterization », *International Journal of Polymer Science*, 2013. https://www.hindawi.com/journals/ijps/2013/514951/ (consulté le janv. 31, 2020).

[41] T. Sakai, T. Morikiyo, C. R. Rios-Soberanis, S. Yoneyama, et S. Wakayama, « Effect of Crushing Method of Wasted Tire on Mechanical Behavior on PLA Composites », in *Challenges in Mechanics of Time-Dependent Materials and Processes in Conventional and Multifunctional Materials, Volume 2*, New York, NY, 2013, p. 85-91, doi: 10.1007/978-1-4614-4241-7_13.

[42] J. Yang, S. Nie, et J. Zhu, « A comparative study on different rubbery modifiers: Effect on morphologies, mechanical, and thermal properties of PLA blends », *J. Appl. Polym. Sci.*, vol. 133, nº 17, 2016, doi: 10.1002/app.43340.

[43] J. Yang, S.-B. Nie, G.-X. Ding, Z.-F. Wang, J.-S. Gao, et J.-B. Zhu, « Mechanical Properties, Morphologies and Thermal Decomposition Kinetics of Poly(lactic acid) Toughened by Waste Rubber Powder », *Int. Polym. Process.*, vol. 30, p. 467-475, août 2015, doi: 10.3139/217.3049.

[44] M. Nematollahi, A. Jalali-Arani, et H. Modarress, « High-performance bio-based poly(lactic acid)/natural rubber/epoxidized natural rubber blends: effect of epoxidized natural rubber on microstructure, toughness and static and dynamic mechanical properties », *Polym. Int.*, vol. 68, nº 3, p. 439-446, 2019, doi: https://doi.org/10.1002/pi.5727.

[45] X. Lu *et al.*, « Supertoughened Poly(lactic acid)/Polyurethane Blend Material by in Situ Reactive Interfacial Compatibilization via Dynamic Vulcanization », *Ind. Eng. Chem. Res.*, vol. 53, nº 44, p. 17386-17393, nov. 2014, doi: 10.1021/ie503092w.

[46] Y. Chen, D. Yuan, et C. Xu, « Dynamically Vulcanized Biobased Polylactide/Natural Rubber Blend Material with Continuous Cross-Linked Rubber Phase », *ACS Appl. Mater. Interfaces*, vol. 6, nº 6, p. 3811-3816, mars 2014, doi: 10.1021/am5004766.

[47] G. Kraus, « Swelling of filler-reinforced vulcanizates », *J. Appl. Polym. Sci.*, vol. 7, nº 3, p. 861-871, 1963, doi: https://doi.org/10.1002/app.1963.070070306.

[48] N. Candau, « Compréhension des mécanismes de cristallisation sous tension des élastomères en conditions quasi-statiques et dynamiques », These de doctorat, Lyon, INSA, 2014.

[49] N. Candau, L. Chazeau, J.-M. Chenal, C. Gauthier, et E. Munch, « Complex dependence on the elastically active chains density of the strain induced crystallization of vulcanized natural rubbers, from low to high strain rate », *Polymer*, vol. 97, p. 158-166, août 2016, doi: 10.1016/j.polymer.2016.05.020.

[50] N. Candau, O. Oguz, E. Peuvrel-Disdier, J.-L. Bouvard, C. Pradille, et N. Billon, « Strain-induced network chains damage in carbon black filled EPDM », *Polymer*, vol. 175, p. 329-338, juin 2019, doi: 10.1016/j.polymer.2019.05.017.

[51] N. Candau, O. Oguz, E. Peuvrel-Disdier, J.-L. Bouvard, C. Pradille, et N. Billon, « Strain and filler ratio transitions from chains network to filler network damage in EPDM during single and cyclic loadings », *Polymer*, vol. 197, p. 122435, mai 2020, doi: 10.1016/j.polymer.2020.122435.

[52] W. Zefeng, K. Yong, W. Zhao, et C. Yi, « Recycling waste tire rubber by water jet pulverization: powder characteristics and reinforcing performance in natural rubber composites », *J. Polym. Eng.*, vol. 38, nº 1, p. 51-62, janv. 2018, doi: 10.1515/polyeng-2016-0383.

[53] A. N. Gisbert, J. E. C. Amorós, J. L. Martínez, et A. M. Garcia, « Study of Thermal Degradation Kinetics of Elastomeric Powder (Ground Tire Rubber) », *Polym.-Plast. Technol. Eng.*, vol. 47, nº 1, p. 36-39, déc. 2007, doi: 10.1080/03602550701580870.

[54] K. Cheng et Z. Heidari, « Combined interpretation of NMR and TGA measurements to quantify the impact of relative humidity on hydration of clay minerals », *Appl. Clay Sci.*, vol. 143, p. 362-371, juill. 2017, doi: 10.1016/j.clay.2017.04.006.

[55] H. Wang, C. Li, Z. Peng, et S. Zhang, « Characterization and thermal behavior of kaolin », *J. Therm. Anal. Calorim.*, vol. 105, nº 1, p. 157-160, mars 2011, doi: 10.1007/s10973-011-1385-0.

[56] G. R. Hamed, « Molecular Aspects of the Fatigue and Fracture of Rubber », *Rubber Chem. Technol.*, vol. 67, nº 3, p. 529-536, juill. 1994, doi: 10.5254/1.3538689.

[57] N. Candau *et al.*, « Effect of the Strain Rate on Damage in Filled EPDM during Single and Cyclic Loadings », *Polymers*, vol. 12, nº 12, Art. nº 12, déc. 2020, doi: 10.3390/polym12123021.

[58] N. Candau *et al.*, « Heat source and voiding signatures of Mullins damage in filled EPDM », *Polym. Test.*, vol. 91, p. 106838, nov. 2020, doi: 10.1016/j.polymertesting.2020.106838.

[59] J. L. Valentín, A. Fernández-Torres, P. Posadas, A. Marcos-Fernández, A. Rodríguez, et L. González, « Measurements of freezing-point depression to evaluate rubber network structure. Crosslinking of natural rubber with dicumyl peroxide », *J. Polym. Sci. Part B Polym. Phys.*, vol. 45, nº 5, p. 544-556, 2007, doi: https://doi.org/10.1002/polb.21060.

[60] J. L. Valentín *et al.*, « Novel Experimental Approach To Evaluate Filler−Elastomer Interactions », *Macromolecules*, vol. 43, nº 1, p. 334-346, janv. 2010, doi: 10.1021/ma901999j.

[61] M. Myhre et D. A. MacKillop, « Rubber Recycling », *Rubber Chem. Technol.*, vol. 75, nº 3, p. 429-474, juill. 2002, doi: 10.5254/1.3547678.

[62] M. L. Maspoch Rulduà *et al.*, « Ductile-brittle transition behaviour of PLA/o-MMT films during the physical aging process », *Express Polym. Lett.*, 2015.

[63] N. Najafi, M. C. Heuzey, et P. J. Carreau, « Polylactide (PLA)-clay nanocomposites prepared by melt compounding in the presence of a chain extender », *Compos. Sci. Technol.*, vol. 72, nº 5, p. 608-615, mars 2012, doi: 10.1016/j.compscitech.2012.01.005.

[64] B. Coppola, N. Cappetti, L. Di Maio, P. Scarfato, et L. Incarnato, « 3D Printing of PLA/clay Nanocomposites: Influence of Printing Temperature on Printed Samples Properties », *Materials*, vol. 11, nº 10, Art. nº 10, oct. 2018, doi: 10.3390/ma11101947.

[65] S. Yang, Z.-H. Wu, W. Yang, et M.-B. Yang, « Thermal and mechanical properties of chemical crosslinked polylactide (PLA) », *Polym. Test.*, vol. 27, nº 8, p. 957-963, déc. 2008, doi: 10.1016/j.polymertesting.2008.08.009.

[66] G. Stoclet, J. M. Lefebvre, R. Séguéla, et C. Vanmansart, « In-situ SAXS study of the plastic deformation behavior of polylactide upon cold-drawing », *Polymer*, vol. 55, nº 7, p. 1817-1828, avr. 2014, doi: 10.1016/j.polymer.2014.02.010.